The Astrophysical Journal Letters, 708:L36–L41, 2010 January 1 doi:10.1088/2041-8205/708/1/L36

ENVIRONMENT OF MAMBO GALAXIES IN THE COSMOS FIELD*

M. Aravena[1,2,3], F. Bertoldi[2], C. Carilli[4], E. Schinnerer[5], H. J. McCracken[6], M. Salvato[7], D. Riechers[7,10], K. Sheth[8], V. Smolčić[7], P. Capak[8], A. M. Koekemoer[9], and K. M. Menten[3]

[1] National Radio Astronomy Observatory. 520 Edgemont Road, Charlottesville VA 22903, USA; maravena@nrao.edu
[2] Argelander Institut für Astronomie. Auf dem Hügel 71, 53121 Bonn, Germany
[3] Max-Planck Institut für Radioastronomie. Auf dem Hügel 69, 53121 Bonn, Germany
[4] National Radio Astronomy Observatory, P.O. Box O, Socorro, NM 87801, USA
[5] Max-Planck-Institut für Astronomie, Königstuhl 17, D-69117 Heidelberg, Germany
[6] Institut d'Astrophysique de Paris, 98bis boulevard Arago, 75014 Paris, France
[7] California Institute of Technology, 1200 East California Boulevard, Pasadena, CA 91125, USA
[8] Spitzer Science Center, Caltech, Pasadena, CA 91125, USA
[9] Space Telescope Science Institute, 3700 San Martin Drive, Baltimore, MD 21218, USA
Received 2009 July 27; accepted 2009 November 20; published 2009 December 16

ABSTRACT

Submillimeter galaxies (SMGs) represent a dust-obscured high-redshift population undergoing massive star formation activity. Their properties and space density have suggested that they may evolve into spheroidal galaxies residing in galaxy clusters. In this Letter, we report the discovery of compact ($\sim$10″–20″) galaxy overdensities centered at the position of three SMGs detected with the Max-Planck millimeter bolometer camera in the COSMOS field. These associations are statistically significant. The photometric redshifts of galaxies in these structures are consistent with their associated SMGs; all of them are between $z = 1.4$ and 2.5, implying projected physical sizes of $\sim$170 kpc for the overdensities. Our results suggest that about 30% of the radio-identified bright SMGs in that redshift range form in galaxy density peaks in the crucial epoch when most stars formed.

Key words: galaxies: clusters: general – galaxies: evolution – galaxies: high-redshift – galaxies: starburst

1. INTRODUCTION

Submillimeter galaxies (SMGs) are dust-obscured starburst galaxies at high redshift (Smail et al. 1997; Hughes et al. 1998; Barger et al. 1998). Their large dynamical (Greve et al. 2005; Tacconi et al. 2006, 2008) and stellar masses (Borys et al. 2005; Dye et al. 2008), as well as their number densities and clustering properties (Scott et al. 2002; Blain et al. 2004; Viero et al. 2009), suggest they could be the progenitors of present-day luminous ellipticals (Lilly et al. 1999; Swinbank et al. 2006). Some SMGs are known to be associated with galaxy clusters at high redshifts (e.g., Webb et al. 2005) and to be located in extended overdensities of LBGs and radio galaxy fields (Ivison et al. 2000; Smail et al. 2003; Stevens et al. 2003; Chapman et al. 2009; Daddi et al. 2009; Tamura et al. 2009).

If SMGs are progenitors of massive clustered spheroids, they would likely show signs of clustering in the epoch when these galaxies have their peak in activity and luminosity ($z \sim 1$–3), similar to what is observed for powerful active galactic nuclei (AGNs; Miley & De Breuck 2008). Attempts to measure the clustering of SMGs indicate that they are associated with massive dark matter halos and possibly trace the largest scale structures at high redshifts (Blain et al. 2004; Viero et al. 2009; Weiss et al. 2009). However, current submillimeter blank-field surveys either cover small areas in the sky, yielding a few tens of sources within contiguous fields (Coppin et al. 2006; Bertoldi et al. 2007; Scott et al. 2008; Perera et al. 2008; Austermann et al. 2009), or are limited by poor angular resolution albeit covering large regions (Devlin et al. 2009). Hence, good quantitative studies of the small- to large-scale clustering of the SMG population are not feasible until large surveys comprising a few square degrees on the sky under good resolution ($\lesssim$20″) can be made.

Studies of the environment of SMGs are possible when utilizing the rich complementary data available for current (sub)millimeter fields. Whether SMGs are embedded in regions with an enhanced number of optical/near-IR detected high-redshift galaxies has yet not been quantified. In this Letter, we investigate to what extent SMGs are located in clustered fields. For this, we make use of deep optical and near-IR imaging data in the central part of the COSMOS field to measure the density of high-redshift BzK galaxies in the surroundings of SMGs. This allows us to study the relation of blank-field detected SMGs with the most prominent galaxy density peaks at high redshift. Hereafter, we assume a cosmology with $H_0 = 70$ km s^{-1} Mpc^{-1}, $\Omega_\Lambda = 0.7$ and $\Omega_M = 0.3$ and use all magnitudes in the AB system.

2. OBSERVATIONS

2.1. COSMOS Photometric Data

The COSMOS survey (Scoville et al. 2007) covers a sufficiently large area, 1.°4 × 1.°4, at appropriate depth over nearly the entire electromagnetic spectrum to provide a comprehensive view of galaxy formation and large-scale structure.

The COSMOS i^+-band selected photometric catalog includes a total of 30 narrow, intermediate and broadband filters covering from UV to mid-IR wavelengths that allowed the computation of accurate photometric redshifts down to $i^+_{\rm AB} = 26.5$ (see Ilbert et al. 2009; Salvato et al. 2009).

A new deep K-band survey covering the entire COSMOS field was recently carried out by McCracken et al. (2009). The K-band image reaches seeing values of $\sim$0.″7 with variations of

* Based on observations obtained, within the COSMOS Legacy Survey, with the IRAM 30 m, NRAO-VLA, *Hubble Space Telescope* (*HST*), Canada–France–Hawaii Telescope (CFHT), Subaru, KPNO, Cerro Tololo Inter-American Observatory (CTIO), and ESO Observatories. The National Radio Astronomy Observatory is a facility of the National Science Foundation (NSF), operated under cooperative agreement by Associated Universities Inc.

[10] Hubble fellow.

less than ∼20% across the entire COSMOS field. The *K*-band selected catalog includes the B^+, z^+, and i^+ bands, reaching a completeness limit $K_{AB} \approx 23.0$ and a 1σ limit in the $2''$ diameter aperture of 25.4 (for details, see McCracken et al. 2009). About 85% of the sources detected in this *K*-band image down to $K = 23.0$ have a photometric redshift estimate based on the i^+-band photometric redshift catalog.

The optical/IR imaging was supplemented with deep Very Large Array (VLA) 1.4 GHz radio imaging (Schinnerer et al. 2004, 2007; Bondi et al. 2008) for the full COSMOS area to an average rms level of 10 μJy at a resolution of $1\farcs5$.

2.2. MAMBO 1.2 mm Observations

An effective area of $\sim 22' \times 22'$ of the COSMOS field was mapped at 1.2 mm by Bertoldi et al. (2007) using the Max-Planck millimeter bolometer camera (MAMBO) at the Institut de Radioastronomie Millimétrique (IRAM) 30 m telescope. The COSMOS MAMBO (COSBO) survey is centered at (R.A., decl.) = ($10^h00^m30^s$, $02°12'00''$) and reaches a noise level of 1.0 mJy per $11''$ beam.

Fifteen millimeter sources were detected with a significance $>4\sigma$. Eleven of them were found to have a significant 1.4 GHz VLA counterpart. Additional 12 lower significance sources (3.5–4.0σ) were selected based on their association with radio sources within $5''$ from the millimeter position (Bertoldi et al. 2007). Two more MAMBO sources with signal-to-noise ratio, S/N = 3–4σ were selected based on their match with significant 1.1 mm Bolocam (J. Aguirre et al. 2010, in preparation) and radio sources.

3. ENVIRONMENT OF SUBMILLIMETER GALAXIES

3.1. BzK Selection

The *BzK* color–color criterion (Daddi et al. 2004) provides an efficient way to select galaxies in the crucial epoch when star formation and SMG activity are peaked (z = 1–3).

Figure 1 shows the *BzK* color–color diagram for the *K*-band selected counterparts to the MAMBO sources and for objects with $K < 23$ in the COSBO field. Small corrections account for the difference between the VLT *B* band used in the original *BzK* criterion and our B_J band (McCracken et al. 2009). According to this, sources with $BzK \equiv (z-K)-(B-z) > -0.2$ are star-forming galaxies at redshift >1.4 (s*BzK*), while objects with $BzK < -0.2$ but $(z-K) > 2.5$ are old passively evolving galaxies at redshift >1.4 (p*BzK*). Objects with $BzK < -0.2$ and $(z-K) < 2.5$ correspond to a mixture of old and star-forming galaxies at redshift <1.4 (n*BzK*). The restriction $(z-K) < 0.3(B-z) - 0.5$ allows the separation of stars.

To study the environment of the MAMBO galaxies, we used the *BzK* criteria to create a *K*-band selected galaxy sample containing a mixture of passive and star-forming galaxies at high redshift. We constrained our sample to include objects in the magnitude range K = 17–23 and used the *BzK* criterion to reject stars.

We note that while the *BzK* criterion is very efficient selecting galaxies at $z > 1.4$, with ∼90% completeness down to $K = 23$ (based on spectroscopic measurements; Barger et al. 2008), it still suffers a great degree of contamination (∼36%), mostly from sources at z = 1.0–1.4 (∼30%; Barger et al. 2008). Only a small percentage (∼10%) appears to lie at $z < 1$ and $z > 3$.

3.2. Projected Density Distribution

We constructed number density maps of high-redshift *BzK* galaxies in the COSBO field. For this, we created a grid of 200×200 positions equally spaced by $7''$ centered at the COSBO field position, and computed the density from the distance to the seventh nearest neighbor *BzK* galaxy, d_7, to each grid point. The density is thereby computed as $n_7 = 7/\pi(d_7)^2$.

This procedure is similar to the one introduced by Dressler (1980). The choice of 7 is a compromise between accounting for structures on small scales (groups of $\gtrsim 4$ galaxies around SMGs) and good statistics for each density value. Similar approaches have been applied to known rich galaxy clusters (e.g., Guzzo et al. 2007), but using photometric or spectroscopic information to compute the number density in redshift slices.

Figure 2 shows the projected number density map of high-redshift *BzK* galaxies in the COSBO field. The average and standard deviation values were computed by using all grid points from our density map (Figure 2). The average density thus computed is 7.0 ± 4.6 arcmin^{-2} ($K < 23.0$), where the quoted uncertainty corresponds to the actual cosmic variance. Down to $K = 21.8$, we find an average density of 1.5 ± 1.0 arcmin^{-2}, which compares well with the number counts of high-redshift *BzK* galaxies in other surveys at this depth (Kong et al. 2006).

We find that four MAMBO galaxies (COSBO 1, 3, 6, and 16) are embedded in significant overdensities (>4σ) of high-redshift *BzK* galaxies. All the galaxies in these overdensities are star-forming rather than passive evolving galaxies. Three out of these four SMGs were detected with S/N >4 in the MAMBO map (Bertoldi et al. 2007). The overdensities of galaxies around MAMBO sources can also be seen directly on the optical and IR images (Figure 3). Here, red galaxies are easily distinguished, showing an excess toward the MAMBO source position (image center). The typical radial extent of these overdensities is ∼5″–10″ (∼20″ in diameter). At a redshift of ∼2, this implies structures on scales of ∼170 kpc, similar to what has been found for QSO and radio galaxy fields (Hall & Green 1998; Best 2000).

3.3. Probability of Chance Association

To estimate the probability P that an overdensity is found by chance within a distance d from a MAMBO galaxy, we performed Monte Carlo simulations of significant density peaks drawn by the underlying distribution of overdensities in the COSBO field.

To identify all the peaks in our density map, we used the IDL version of the DAOPHOT task FIND. This routine finds the positive perturbations in the density map, and uses marginal Gaussian fits to locate the centroid and amplitude of the density peak. This Gaussian approximation may not be valid for fragmented density structure; however, it is reliable to detect the most significant overdensities which are typically non-fragmented.

Based on this procedure, we found 45 detections with S/N >4, nine of them with S/N $\gtrsim$ 10. Using their observed spatial distribution, we generated 45 peaks in each of the 10,000 samplings, and thereby computed P as the fraction of SMG–overdensity associations in our simulations (Table 1). In the cases of COSBO 3, 6, and 16, the probabilities of chance association are negligible.

3.4. Photometric Redshifts and Comments on Individual Associations

To measure the clustering of the star-forming high-redshift galaxies associated with SMGs in redshift space, we used the COSMOS i^+-band selected photometric redshift catalog (Ilbert

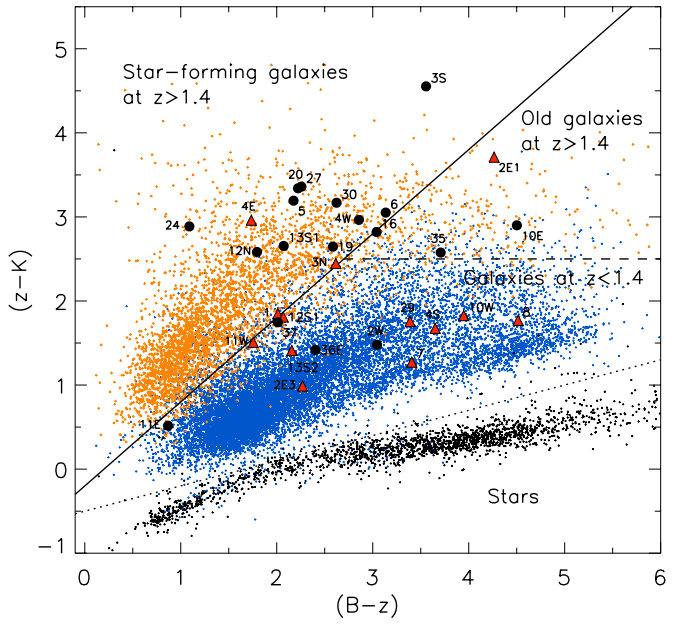

Figure 1. *BzK* diagram for MAMBO sources in the COSMOS field. Reliable *K*-band selected identifications are represented by filled black circles, and ambiguous or unreliable identifications are shown as filled red triangles. The *BzK* loci for galaxies are shown as small crosses. Their color coding (orange, blue, and black) is based on the photometric redshifts ($z > 1.4$, $z < 1.4$, and stars, respectively). The solid line separates star-forming galaxies at $z > 1.4$, while the dashed line separates old passive evolving galaxies at $z > 1.4$. The dotted line separates stars (black) from a mixed population of galaxies at $z < 1.4$.

et al. 2009). The accuracy of these photometric redshifts for faint galaxies ($i^+ \gtrsim 25.5$) is $\sigma \sim 0.2$.

Figure 4 shows the redshift distribution of *K*-band selected galaxies that lie close to the high-redshift *BzK* density peaks associated with SMGs. Since the i^+-band catalog is too shallow to include the obscured optical emission from the MAMBO galaxies, we used the previous photometric redshift estimates from Bertoldi et al. (2007).

For COSBO-1, a recent Submillimetre Array (SMA) detection (which will be published elsewhere) indicates that the millimeter emission is produced by a radio and optically undetected galaxy at $z > 3.5$ (as also implied by its radio-to-millimeter spectral index; Bertoldi et al. 2007). The counterpart to this MAMBO source selected by Bertoldi et al. (2007), a relatively bright Infrared Array Camera (IRAC)/optical source with a photometric redshift of ≈ 1.2, is related to the galaxy group at this redshift. However, it is very probably not responsible for the millimeter emission. The association between this source and

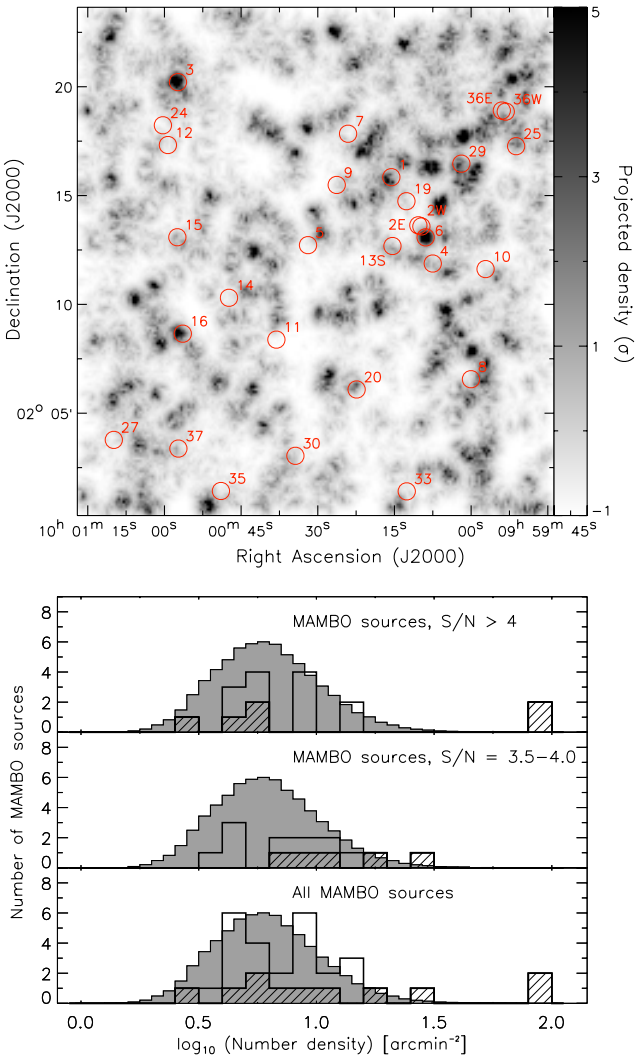

Figure 2. Top: projected number density of high-redshift *BzK* galaxies in the COSBO field ($K < 23$). The gray scale represents the density map given in terms of the standard deviation σ with respect to the average background level. Red circles mark the position of the MAMBO galaxies. ID numbers are the same as in Bertoldi et al. (2007). Bottom: distribution of densities of high-redshift *BzK* galaxies at the position of MAMBO sources (solid) and MAMBO sources with photometric redshifts in the range 1.4–2.5 (solid hatched) compared to the distribution of densities of *BzK* galaxies obtained from the 200×200 grid points in the COSBO density map (shaded).

the overdensity is unlikely, $P_d \sim 0.05$. Hence, we discard this one as a real association between a SMG and a galaxy group at

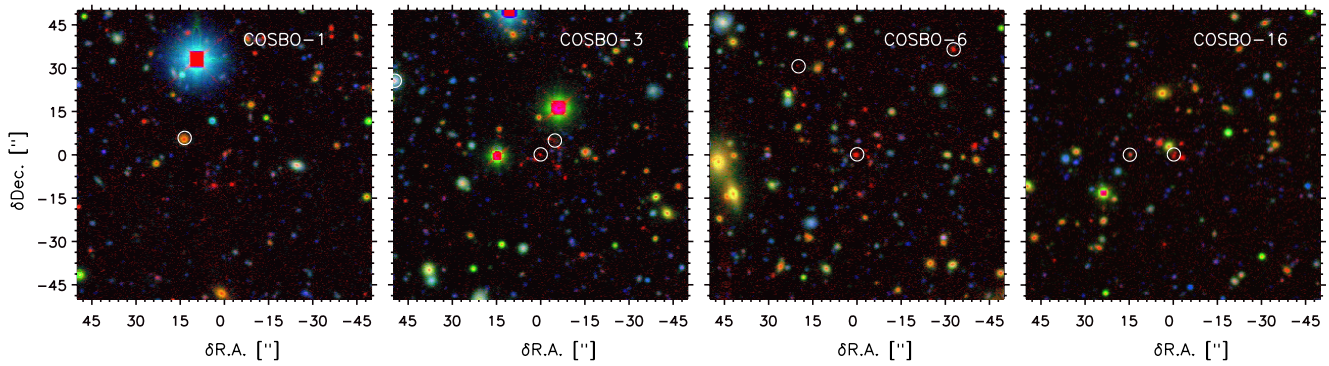

Figure 3. *BzK* color images of MAMBO galaxy fields that are related to strong overdensities of high-redshift galaxies. The images are centered at the MAMBO source position. White circles show the position of significant VLA 1.4 GHz sources.

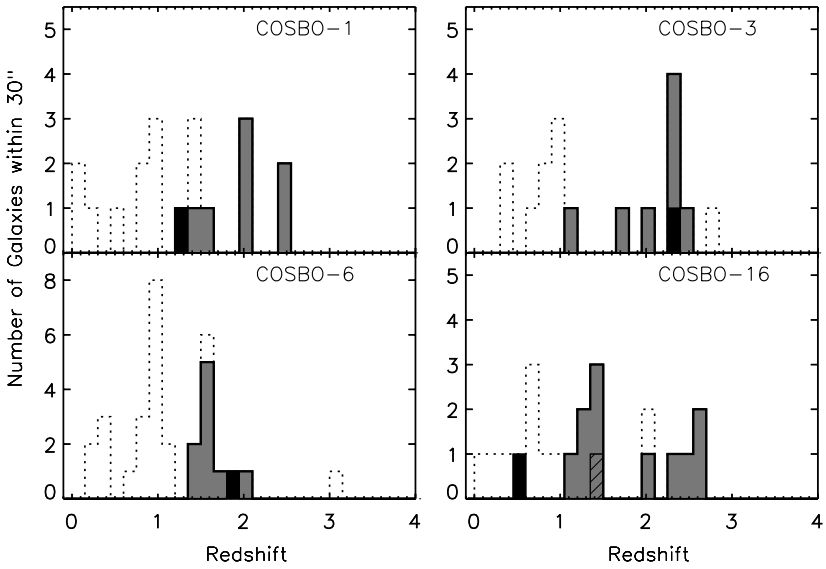

Figure 4. Redshift distribution for galaxies located within 30″ from the density peak of high-redshift galaxies near MAMBO sources. The dotted histogram shows the photometric redshifts for our *K*-band selected galaxies, the dark-gray histogram shows the redshifts for the *K*-band selected high-redshift *BzK* galaxies, and the black single object shows the redshift of the most likely counterpart to the MAMBO source as given by Bertoldi et al. (2007). For COSBO-16, the hashed entry represents the secondary solution from the photometric redshift computation.

Table 1
Associations between High-redshift *BzK* Galaxy Overdensities with Millimeter Sources

ID	R.A.[a]	Decl.[a]	$N^{b}_{30''}$	S/N[c]	d^{d}	$P^{e}_{30''}$	P^{f}_{d}	z^{g}_{median}	z^{h}_{SMG}
	(J2000)				(″)	$\times 10^{-2}$	$\times 10^{-2}$		
COSBO-1	150.0679	2.26209	9	4.6	13.8	18.5	4.7	2.0	1.2
COSBO-3	150.2379	2.33649	10	27.8	2.8	3.9	0.05	2.3	2.3
COSBO-6	150.0357	2.21871	11	22.9	4.6	12.3	0.2	1.6	1.9
COSBO-16	150.2360	2.14549	12	7.2	6.5	12.7	0.7	1.5	0.5

Notes. [a] Position of the density peak. [b] Number of high-redshift *BzK* galaxies within 30″. [c] Peak S/N of the density peak. [d] Distance from the COSBO source to the density peak. [e and f] Probability that a significant overdensity lies by chance within a distance of 30″ and of *d*″ from the MAMBO source. [g] Median photometric redshift for *BzK* galaxies within 30″. [h] Photometric redshift for the SMG from Bertoldi et al. (2007).

$z \sim 1.5$. In cases when the group is at low redshift, gravitational lensing of a faraway SMG is a possibility.

For COSBO-3, the redshift distribution of the galaxies in its close neighborhood is consistent with most of them being at $z \sim 2.2$–2.4 (Figure 4). Two radio sources can be identified within 10″ from the MAMBO source. The most likely radio/IR/optical counterpart (COSBO-3S) has a photometric redshift of 2.3 (Bertoldi et al. 2007). Based on the i^{+}-band selected catalog, we find a redshift of 2.4 for this source, consistent with the likely redshift of the galaxy group. Recent CARMA observations indicate the MAMBO emission is produced by at least two sources (V. Smŏlcić et al. 2010, in preparation).

Most galaxies in the group around COSBO-6 lie at $z \sim 1.2$–1.8. Bertoldi et al. (2007) estimated a photometric redshift of 1.9 for the radio/optical identified counterpart to the millimeter emission. Although the redshift for the likely counterpart is slightly larger than the one implied by the redshift distribution of the surrounding high-redshift *BzK* galaxies, it agrees within $\Delta z = 0.2$.

The galaxies surrounding COSBO-16 have a photometric redshift of ∼1.4. The photometric redshift derived for the likely radio/optical counterpart from the i^{+}-band selected catalog is ≈0.5 (Bertoldi et al. 2007); however, the secondary solution (second minima in the χ^2 distribution) implies $z \sim 1.4$. The photometric redshift listed in the COSMOS catalog is, however, 2.55 which agrees better with that implied by the radio-to-millimeter spectral index (Bertoldi et al. 2007). Because of the somewhat ambiguous redshift derivation for the millimeter source, it is difficult to relate it to the redshift peak in the surrounding galaxies, although we may slightly favor to use $z = 1.4$ as the most likely case for both.

4. SUMMARY AND DISCUSSION

We find that significant overdensities of star-forming high-redshift galaxies are related to three MAMBO galaxies detected in the COSMOS field. These groups are compact in size, and the peaks of their redshift distributions are compatible with the redshift estimated for the associated MAMBO galaxies.

4.1. SMGs in Dense Environments

If SMGs are related to the formation of structures at high redshift, we would expect that most SMGs are located in regions with enhanced galaxy densities. However, only a few SMGs in our sample can be associated with strong galaxy overdensities. This could be partly attributed to a selection effect, since we are comparing the overall population of SMGs at various redshifts with *K*-band selected galaxies in the range $z \sim 1.4$–2.5. According to Chapman et al. (2005), ∼55% of the radio-identified, bright SMG population lies in this redshift

range. From our sample of 15 MAMBO sources detected with a significance $>4\sigma$, 11 were identified to have a radio counterpart. Following Chapman et al., we estimate that about 6 of these 11 MAMBO sources should be at $z = 1.4$–2.5, while using the photometric redshifts reported by Bertoldi et al. (2007), 7 appear to lie in this redshift range. This implies that ∼30% of the radio-identified, significant MAMBO sources at $z = 1.4$–2.5 are associated with substantial overdensities of massive galaxies at these redshifts.

Note that our study is biased in that we are selecting massive galaxies at $z = 1.4$–2.5. Our $K < 23$ limit roughly translates into stellar masses $\gtrsim (2\text{–}4) \times 10^{10}\, M_{\odot}$ (Daddi et al. 2004), and therefore we miss less massive galaxies that could be associated with SMGs at these redshifts. However, the fact remains that only a fraction of the SMGs are related to groups of massive galaxies in the crucial epoch of galaxy assembly.

We compared the distribution of densities at the position of $>4\sigma$ MAMBO source detections with the distribution of densities of *BzK* galaxies in the field (Figure 2). A Kolmogorov–Smirnov (K–S) test does not reject the null hypothesis that both samples follow the same distribution at a 46% significance level. Restricting the $>4\sigma$ MAMBO source sample to sources at $z = 1.4$–2.5, the K–S test does not reject the null hypothesis at a 43% level. This is somewhat inconsistent with the fact that two of the brightest MAMBO galaxies are related to some of the strongest overdensities in the field; however, it may merely reflect the low number of SMGs that we used to compute the K–S statistic. For the 3.5σ–4.0σ MAMBO source sample, the K–S test does not rule out the null hypothesis at a 23% level, whereas if we limit this sample to galaxies with $z = 1.4$–2.5, the K–S test gives a 3.4% significance level. This strongly suggests that the densities at the position of the fainter MAMBO sources follow a different distribution from that of *BzK* galaxies in the field. For both samples combined (all MAMBO sources), the K–S test gives only a 9.6% probability that they follow the same distribution of densities of *BzK* galaxies in the field, which is similar to the value that we obtain if we restrict the sample to $z = 1.4$–2.5, 12.6%, again suggesting that the distributions are different.

Overall, our results show that only a fraction (30%) of MAMBO sources at $z = 1.4$–2.5 is located in strongly overdense regions. This suggests that only some SMGs are linked to the formation of structures at high redshift. Although we find a hint that some SMGs could be located in environments denser than that of the general population of galaxies at $z \sim 2$, it is not possible to discern whether this is a real trend or is due to cosmic variance as our analysis is based only on a handful of SMGs.

The presence of bright SMGs in galaxy overdensities is possibly related to the fact that the density peaks of high-redshift *BzK* galaxies associated with MAMBO galaxies (e.g., for COSBO-3 and 6) are the strongest in the whole COSBO area. Denser groups of star-forming *BzK* galaxies are more likely to produce major mergers between galaxies and thus are prone to trigger violent star formation activity. The merger of two gas-rich *BzK* galaxies close to the center of a galaxy group could induce a starburst that would be seen as a bright SMG. Star-forming *BzK* galaxies have large reservoirs of molecular gas ($\sim 10^{11}\, M_{\odot}$; Daddi et al. 2008), and could easily sustain the typical star formation rates observed in SMGs ($\sim 1000\, M_{\odot}\ \mathrm{yr}^{-1}$) for $\lesssim$100 Myr. The densest galaxy groups are thus ideal for the formation of bright submillimeter activity.

4.2. Comparison with Other Studies

Similar studies relating the distribution of SMGs with the large-scale structures traced by optically selected galaxies at high redshift have recently been done. In particular, Tamura et al. (2009) found a strong overdensity of SMGs toward a massive protocluster of Lyα emitters at $z = 3.1$, reflecting a strong link between SMGs and the large-scale structure. Nevertheless, this study is based on a proto-cluster field where we know that strong clustering is taking place.

Studies of the galaxy–galaxy angular correlation function in blank fields indicate that SMGs and IR luminous galaxies at $z \sim 2$ are clustered on typical angular scales of 15″–25″, being related to massive dark matter halos ($\sim 10^{13}\, M_{\odot}$; Blain et al. 2004; Greve et al. 2004; Scott et al. 2006; Farrah et al. 2006; Viero et al. 2009; Weiss et al. 2009). Our results are consistent with these results in that strong clustering between SMGs and *BzK* galaxies occur on similar angular scales. We note, however, that studies purely based on the angular two-point correlation function are only able to measure the average clustering properties of SMGs. They miss the important fact that not all the SMGs are located in clustered environments, as we find in this Letter, and therefore only a few of them will significantly contribute to the clustering signal of the angular correlation function in small scales.

M. Aravena was partly supported for this research through a stipend from the International Max-Planck Research School (IMPRS) for Radio and Infrared Astronomy at the Universities of Bonn and Cologne. D. Riechers acknowledges support from NASA through Hubble Fellowship grant HST-HF-01212.01A awarded by the STScI, operated by AURA, under contract NAS 5-26555.

REFERENCES

Austermann, J. E., et al. 2009, MNRAS, in press (arXiv:0907.1093)
Barger, A. J., Cowie, L. L., & Wang, W.-H. 2008, ApJ, 689, 687
Barger, A. J., et al. 1998, Nature, 394, 248
Bertoldi, F., et al. 2007, ApJS, 172, 132
Best, P. N. 2000, MNRAS, 317, 720
Blain, A. W., Chapman, S. C., Smail, I., & Ivison, R. 2004, ApJ, 611, 725
Bondi, M., et al. 2008, ApJ, 681, 1129
Borys, C., et al. 2005, ApJ, 635, 853
Chapman, S. C., Blain, A. W., Smail, I., & Ivison, R. J. 2005, ApJ, 622, 772
Chapman, S. C., et al. 2009, ApJ, 691, 560
Coppin, K., et al. 2006, MNRAS, 372, 1621
Daddi, E., et al. 2004, ApJ, 617, 746
Daddi, E., et al. 2008, ApJ, 673, L21
Daddi, E., et al. 2009, ApJ, 694, 1517
Devlin, M. J., et al. 2009, Nature, 458, 737
Dressler, A. 1980, ApJ, 236, 351
Dye, S., et al. 2008, MNRAS, 386, 1107
Farrah, D., et al. 2006, ApJ, 641, L17
Greve, T. R., et al. 2004, MNRAS, 354, 779
Greve, T. R., et al. 2005, MNRAS, 359, 1165
Guzzo, L., et al. 2007, ApJS, 172, 254
Hall, P. B., & Green, R. F. 1998, ApJ, 507, 558
Hughes, D. H., et al. 1998, Nature, 394, 241
Ilbert, O., et al. 2009, ApJ, 690, 1236
Ivison, R. J., et al. 2000, ApJ, 542, 27
Kong, X., et al. 2006, ApJ, 638, 72
Lilly, S., et al. 1999, ApJ, 518, 641
McCracken, H. J., et al. 2009, arXiv:0910.2705
Miley, G., & De Breuck, C. 2008, A&ARv, 15, 67
Perera, T. A., et al. 2008, MNRAS, 391, 1227
Salvato, M., et al. 2009, ApJ, 690, 1250

Schinnerer, E., et al. 2004, AJ, 128, 1974
Schinnerer, E., et al. 2007, ApJS, 172, 46
Scott, K. S., et al. 2008, MNRAS, 385, 2225
Scott, S. E., Dunlop, J. S., & Serjeant, S. 2006, MNRAS, 370, 1057
Scott, S. E., et al. 2002, MNRAS, 331, 817
Scoville, N., et al. 2007, ApJS, 172, 1
Smail, I., Ivison, R. J., & Blain, A. W. 1997, ApJ, 490, 5
Smail, I., et al. 2003, ApJ, 583, 551
Stevens, J. A., et al. 2003, Nature, 425, 264
Swinbank, A. M., et al. 2006, MNRAS, 371, 465
Tacconi, L. J., et al. 2006, ApJ, 640, 228
Tacconi, L. J., et al. 2008, ApJ, 680, 246
Tamura, Y., et al. 2009, Nature, 459, 61
Viero, M. P., et al. 2009, arXiv:0904.1200
Webb, T. M. A., et al. 2005, ApJ, 631, 187
Weiss, A., et al. 2009, arXiv:0910.2821